Materials Science-Poland, Vol. 24, No. 2/1, 2006

Sliding wear, slurry erosive wear, and corrosive wear of aluminium/SiC composite

M. RAMACHANDRA[1*], K. RADHAKRISHNA[2]

[1]Department of Manufacturing Engineering, BMS College of Engineering, Bangalore 560 019, Karnataka, India.

[2]Department of Mechanical Engineering, BMS College of Engineering, Bangalore 560 019, India

In this study, an aluminium based metal matrix was reinforced with silicon carbide (SiC) particulates using the conventional vortex casting technique. Macro- and microstructural studies conducted on the samples revealed a near uniform distribution of SiC particulates. Sliding wear, slurry erosive wear, and corrosive wear of the as-cast metal matrix composite (MMC) were studied. It was found that sliding wear and slurry erosive wear resistance improved considerably with the addition of SiC particles, whereas corrosion resistance decreased. Microscopic examinations of the worn surfaces, wear debris, and subsurface show that the base alloy wears primarily due to micro-cutting. MMCs wear, however, because of micro-cutting, oxidation, plastic deformation, and thermal softening. In slurry erosive wear, the formation of a passive layer retarded the wear of the material. It was observed that pitting corrosion was the dominant mechanism. The bulk hardness increased with an increase in the percentage of SiC particulates. There was not much change in the density of MMCs compared to the base metal.

Key words: *metal matrix composite; MMC; Al-based MMC; SiC; mechanical properties; wear; corrosion*

1. Introduction

The emergence of modern processing techniques, coupled with the need for lighter materials with high strength and stiffness, has catalysed considerable scientific and technological interest in the development of high-performance composite materials as serious competitors to traditionally engineered alloys. The majority of such materials are metallic matrixes reinforced with a high strength, high modulus, and often brittle second phase, in the form of a fibre, particulate, or whiskers embedded in a ductile metal matrix. The reinforced metal matrix offers the potential for a sufficient improvement in efficiency, reliability, and mechanical performance over traditional

*Corresponding author, e-mail: m_rchandra@yahoo.co.in

monolithic alloys. Discontinuously reinforced aluminium matrix composites have emerged from the need for lightweight, highly rigid materials, which are desirable in applications such as high-speed reciprocation. Reinforcement usually comprises particles or whiskers of a ceramic such as silicon carbide, alumina, graphite, etc. A significant increase in stiffness and strength can be conferred with even small reinforcement volume fractions. Many of the applications, for which MMCs are desirable, also require enhanced tribological performance.

The wear resistance of composites has received much attention in the literature, but a direct comparison between findings is often difficult due to specific differences in the wear testing procedure. Work concerning the non-lubricated sliding wear behaviour of such materials has examined a number of variables [1], such as the contact pressure [2–4], sliding velocity [5, 6], temperature [7, 8], particle volume fraction [9, 10], and particle size [11]. A number of mechanisms have been proposed to explain the sliding wear behaviour of these composites, many of which are discussed in a review of the subject [12].

In recent years, considerable interest has been paid in extending the use of these composite materials in the marine environment [13]. This demands an examination of the corrosion as well as erosion–corrosion characteristics of the composite materials under a simulated marine environment. A few studies have been reported by different authors on the erosive–corrosive wear behaviour of Al alloys and composites [14]. It has been reported by a group of authors that the composites exhibit inferior wear resistance to that of alloys under corrosive media [15, 16]. Other groups have reported that composites have higher corrosion and erosive–corrosive wear resistance [17].

In the present investigation, aluminium-based metal matrix composites containing up to 15% weight percentage of SiC particulates, were successfully synthesized using the vortex method. Dry sliding wear, slurry erosive wear, and corrosive wear behaviour of the MMCs was investigated along with some of its mechanical properties.

2. Materials

The matrix material used in the experimental investigation was an aluminium alloy (Si – 7.2%), LM25, whose chemical composition is listed in Table 1. This alloy conforms to BS1490, and its SEM micrograph is shown in Fig. 1. LM25 is mainly used when good mechanical properties are required. It is, in practice, a general-purpose high strength-casting alloy. In its heat-treated form, its tensile strength can be increased from around 130–150 $N \cdot mm^{-2}$ to up to 230–280 $N \cdot mm^{-2}$. Aluminium and silicon alloys have no solid solubility below the eutectic, and the microstructure solidifies in the form of silicon particles in an aluminium matrix. Aluminium–silicon castings have good corrosion resistance and are used in the cases where particularly high strength is required.

Silicon carbide (SiC) used as reinforcement is a highly wear resistant and has good mechanical properties, including high-temperature strength and thermal shock resistance. The SEM micrograph of SiC used in the investigation is shown in Fig. 2. The average particle size was 10 μm, and particles were found to be irregularly shaped.

Table 1. Chemical composition of the aluminium base alloy (wt. %)

Si	Fe	Cu	Mn	Mg	Zn	Al
7.2	0.2	0.23	0.1	0.4	0.1	balance

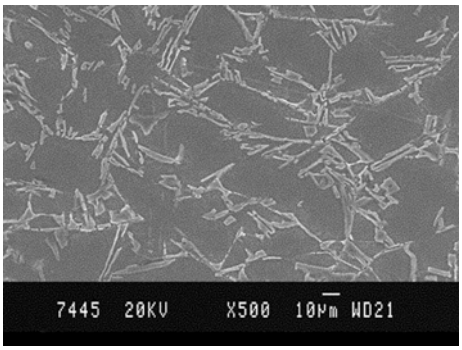

Fig. 1. Matrix material, A – Si 7.2%

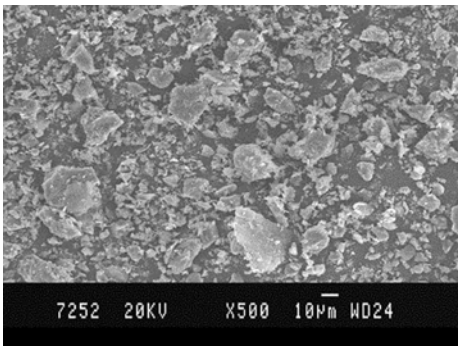

Fig. 2. Micrograph of silicon carbide particles

3. Experimental procedure

Processing. The synthesis of the metal matrix composite used in the present study was carried out by the stir casting method. Al–Si (7.2%) alloys in the form of ingots were used for the trials. The cleaned metal ingots were melted to the desired super heating temperature of 800 °C in graphite crucibles under a cover of flux in order to minimize the oxidation of the molten metal. A three-phase electrical resistance furnace with temperature controlling device was used for melting. For each melting, 3–4 kg of alloy was used. The super heated molten metal was degassed at a temperature of 780 °C. SiC particulates, preheated to around 500 °C, were then added to the molten metal and stirred continuously by a mechanical stirrer at 720 °C. The stirring time was between 5 and 8 minutes, and the impeller speed was 550 rpm. During stirring, magnesium was added in small quantities to increase the wettability of SiC particles. The dispersion of the preheated SiC particulates was achieved in accordance with the vortex method [18]. The melt, with the reinforced particulates, was poured into the dried, coated, cylindrical permanent metallic moulds 80 mm in diameter and 175 mm high. The pouring temperature was maintained at 680 °C. The same molten metal–SiC particle mixture was poured into strip and spiral fluidity dies for fluidity measurements. The melt was allowed to solidify in the moulds. For the purpose of comparison, the base alloy was cast under similar processing conditions.

Heat treatment. The metal matrix composites produced were exposed to solutionising and age hardening heat treatment, as shown in Figure 3. The solutionising treatment was applied for 16 hours at 525 ºC, and age hardening was done for 18 hours at 175 ºC.

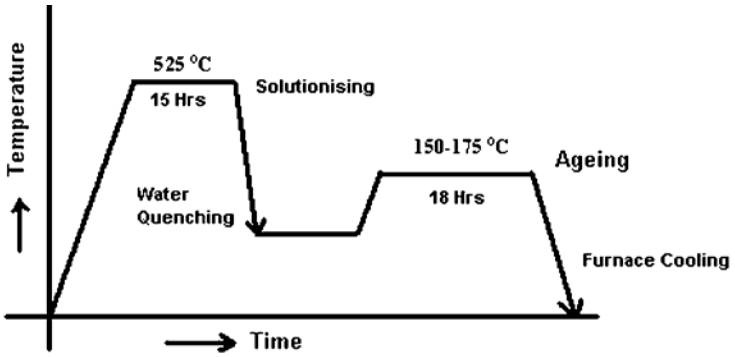

Fig. 3. Solutionising and ageing heat treatment cycle adapted to heat treat MMCs

Density. Density measurements were carried out on the base metal and reinforced samples using Archimedes principle [19]. The buoyant force on a submerged object is equal to the weight of the fluid displaced. This principle is useful for determining the volume and therefore the density of an irregularly shaped object, by measuring its mass in air and its effective mass when submerged in water (density = 1 g·cm^{-3}). This effective mass under water will be its actual mass minus the mass of the fluid displaced. The difference between the real and effective masses therefore gives the mass of the displaced water and allows the volume of the irregularly shaped object to be calculated. Mass divided by the volume thus determined gives a measure of the average density of the object.

Macro- and microstructural characterization. Macrostructural studies were conducted on the as-processed and machined composite castings in order to investigate the distribution of SiC particles retained in the metal matrix. Castings were plain turned on lathe to remove 5 mm of material and reveal the particle distribution on a macroscopic scale.

Microstructural characterization studies were conducted on unreinforced as well as on reinforced samples. This was accomplished by using a scanning electron microscope. The composite samples were metallographically polished prior to examination. Characterization was done in etched conditions. Etching was accomplished using Keller's reagent.

Bulk hardness and microhardness. Bulk hardness measurements were carried out on the base metal and composite samples by using the standard the Brinnel hardness test. The Brinell hardness measurements were carried out in order to investigate the influence of SiC particulate weight fractions on the matrix hardness. The applied load was 500 kgs, and the indenter was a steel ball 10 mm in diameter.

Microhardness measurements were carried out in order to investigate the influence of SiC particles on matrix hardness. The load applied was 50 g, and a Vickers indenter was used. Microhardness measurements were made on the particle and in its vicinity. Round specimens 20 mm in diameter were prepared and polished on differ-

ent grits of emery paper. Averages of 5 readings were taken for both bulk hardness and microhardness measurement.

Sliding wear. Two-body sliding wear tests were carried out on the prepared composite specimens. A computerized pin-on-disc wear test machine was used for these tests. The tangential friction force and wear in microns were monitored with the help of electronic sensors. These two parameters were measured as a function of load, sliding velocity, and per cent of SiC. For each type of material, tests were conducted at three different normal loads (4.9 N, 9.8 N, and 14.7 N), keeping the sliding speed fixed at 95 $m \cdot min^{-1}$. A cylindrical pin 5 mm in diameter and 40 mm long, prepared from composite casting, was loaded through a vertical specimen holder against a horizontal rotating disc. Before testing, the flat surface of a specimen was abraded using 2000 grit paper. The rotating disc was made of carbon steel, with a diameter of 50 mm and hardness of 64 HRC. Wear tests were carried out at room temperature without lubrication for about 140 minutes.

Corrosion wear. The oldest and most wildly used salt spray corrosion testing method was used in the investigation of the corrosive wear of MMCs. A fog of NaCl solution was introduced into a closed chamber, in which specimens were exposed at specific locations. The concentration of the NaCl solution was 3.5%. Corrosive fog was created by bubbling compressed air through hot deionised water. The salt solution was maintained at a temperature of 50 ºC. The specimens for fog corrosion were prepared by cutting specimens $10 \times 20 \times 5$ mm^3 in size from the composite castings. The surfaces of specimens were abraded using 600 grit size emery papers and degreased. Before testing, the specimens were weighed with an accuracy of 0.001 g and exposed to a corrosive atmosphere for a period of 240 h. The specimens were suspended in the corrosive chamber at regular intervals, exposing the abraded surface to salt solution fog. After corrosion testing, the specimens were immersed in Clark's solution for 5 minutes and gently cleaned with a soft brush to remove adhered particles. After drying thoroughly, the specimens were re-weighed to determine weight loss.

Slurry erosive wear. The experimental arrangement for slurry erosive wear consists of a stirrer, which can hold 4 specimens at a time, and a water-cooled pot. All 4 specimens were dipped in a slurry of distilled water and silica sand, and stirred at the speed of 376 $m \cdot min^{-1}$. The slurry was prepared by mixing 80-micron silica sand with distilled water in the ratio 1:2 (pH = 7.1). The slurry wear test was performed at ambient temperature, and the testing time was 14 h.

The specimens for the slurry erosive wear test were cut from composite ingots and plain turned to a diameter of 7 mm. Before testing, specimens were weighed with the accuracy of 0.001 g. After testing, specimens were dried and re-weighed to determine the percentage weight loss.

4. Results and discussion

4.1. Macrostructural and microstructural characterization

Macrostructural studies revealed a reasonably uniform distribution of SiC particles and a slight macro-segregation of particles in some places. The distribution of SiC particles is influenced by the tendency of particles to float due to density differences and interactions with the solidifying metal. It is therefore a strong function of the solidification rate and geometry of castings [20]. The photo macrograph in Figure 4 shows the distribution of SiC particles in a permanent mould cast ingot. A lower concentration of SiC particles was obtained at the top and a higher concentration at the bottom of the castings. The central 70–80% portion of the castings had a near uniform distribution of SiC particles.

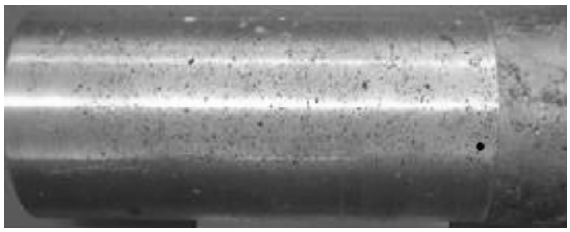

Fig. 4. Photo macrograph of MMC with 15% SiC particles

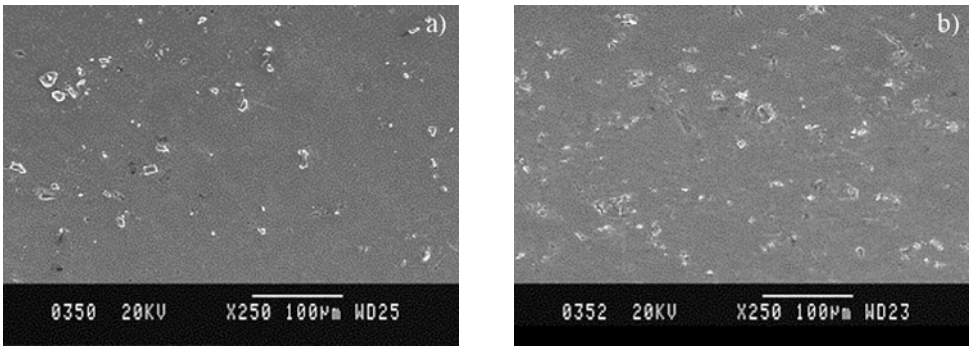

Fig. 5. SEM micrographs of: a) MMC with 5% SiC, b) MMC with 15% SiC particles

Figures 5a and b show the microstructure of MMC with SiC particle distribution in the matrix. The microstructure reveals that there are no voids or discontinuities and a reasonably uniform distribution of SiC particulates. There also was a slight agglomeration of SiC particles in the microscale, but good interfacial bonding between SiC particles and matrix material.

4.2. Fluidity

Fluidity measurements showed that the viscosity increases with increasing SiC content in the molten metal. Figures 6a and b show the photographs of spiral and strip fluidity. Figure 7 shows the results of strip and spiral fluidity. The base metal showed good flowability, and the metal matrix composite with 15% SiC poor flowability in both strip and spiral fluidity.

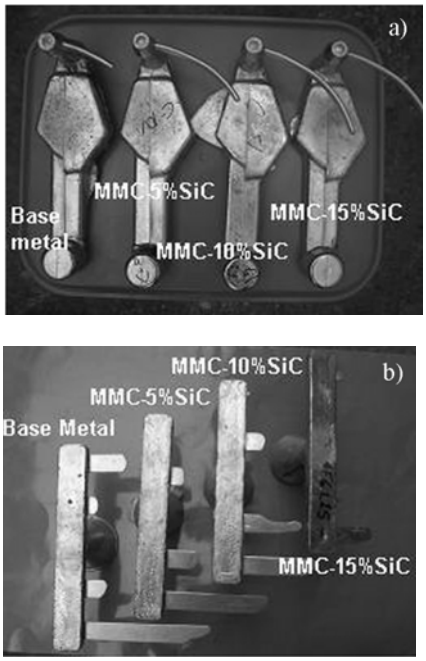

Fig. 6. Spiral fluidity castings (a) and strip fluidity castings (b)

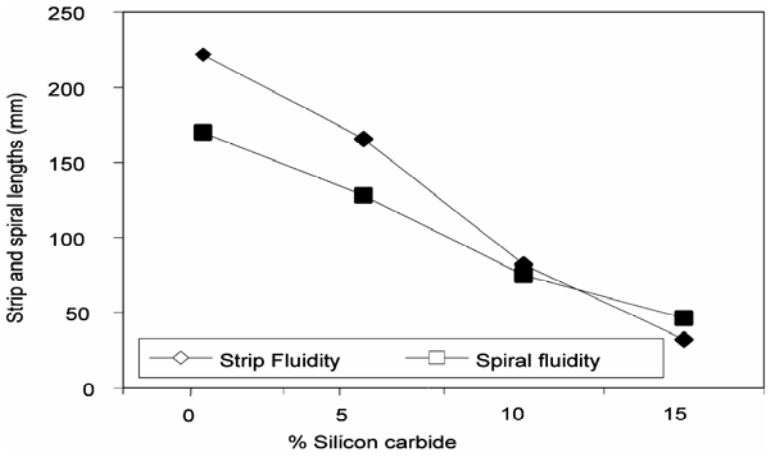

Fig. 7. Strip and spiral lengths for MMC with different SiC particles contents

4.3. Density and hardness measurements

The results of density measurements on the base metal and reinforced materials are shown in Figure 8. The results reveal that the presence of SiC particulates has little effect on the density of the MMCs. Since the density of the reinforced SiC particles is 2580 kg·mm^{-3} – almost the same as that of the base material (2630 kg·mm^{-3}) – not much change in the MMC density was observed.

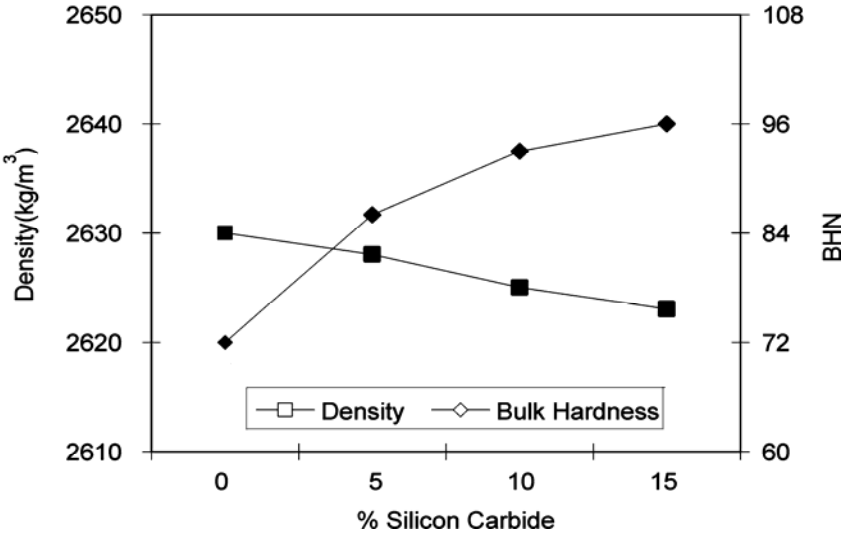

Fig. 8. Variation of density and bulk hardness with SiC contents

The results of microhardness measurements conducted on composite samples containing 15 wt. % of SiC particles are shown in Table 2. The measurements were performed using a 50 g load. The results indicate that hardness varies in the vicinity of SiC particulates, depending on the distance from the interface. The variation, however, does not show a clear trend. The hardness value is higher near the particle–matrix interface as compared to other regions. The lack of a clear trend in the variation of microhardness can be attributed to the influence of neighbouring particles, those beneath and on the sides, on the hardness of the matrix.

Table 2. Microhardness of MMC (SiC – 15 wt. %)

Distance [μm]	Test [Hv]		
	1	2	3
0	524	567	586
10	510	427	560
20	439	435	358
30	310	283	433
40	450	315	183

The results of bulk hardness measurements conducted on the monolithic and reinforced materials are as shown in Figure 8. The results reveal that an increase in the SiC particulate weight percentage in MMC increases the material bulk hardness.

4.4. Sliding wear behaviour

Figure 9 shows the results of the sliding wear behaviour of MMCs with 0%, 5%, 10%, and 15% of SiC. The normal load applied was 14.7 N, and the track velocity was 95 $m \cdot min^{-1}$. In all the test results it is evident that the resistance to wear increases with increasing silicon carbide content. The MMCs with low weight fractions of SiC underwent large wears, and the wear increased almost linearly with time. The base metal exhibits higher wear, and the MMC with 15% SiC showed lower wear.

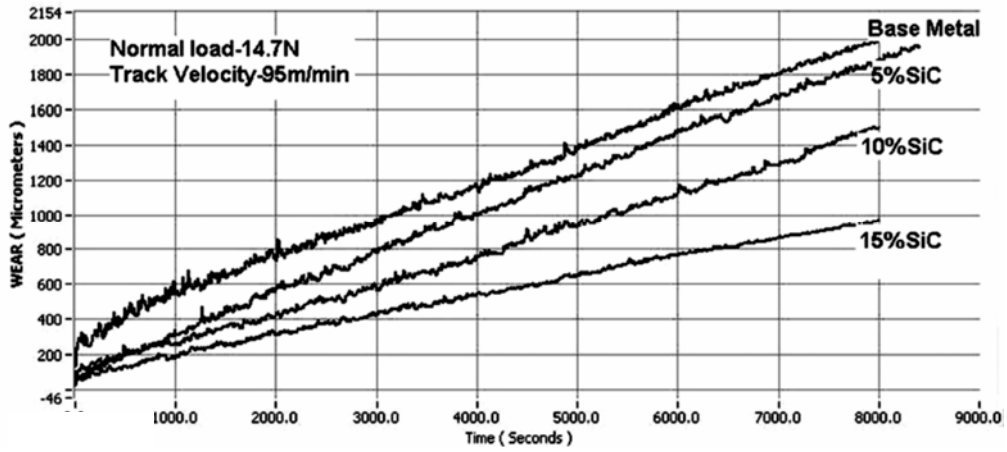

Fig. 9. Sliding wear behaviour of MMCs under different SiC contents

The amount of wear increases with increasing normal load. The sliding wear behaviour of MMC (15%SiC) for various normal loads is shown in Figure 10. With increasing normal load, MMCs underwent a transition from mild to severe wear.

Variation in sliding velocity was achieved by changing the rotational speed of the disc to 500 rpm, 600 rpm, 700 rpm and 800 rpm while keeping the track diameter constant at 30 mm. Figure 11 shows the wear behaviour curves for 15% of SiC MMC for the various sliding velocities. The amount of wear increased with increasing sliding velocity, undergoing a transition from mild to severe wear.

Optical microscopic examinations of the worn pin surfaces identified different wear mechanisms, working either alone or in combination, under the various sliding conditions. These are: abrasion, oxidation, adhesion, and thermal softening. In the following sections, the observed wear mechanisms are discussed in relation to the sliding conditions and wear rates, in order to better understand the tribological characteristics.

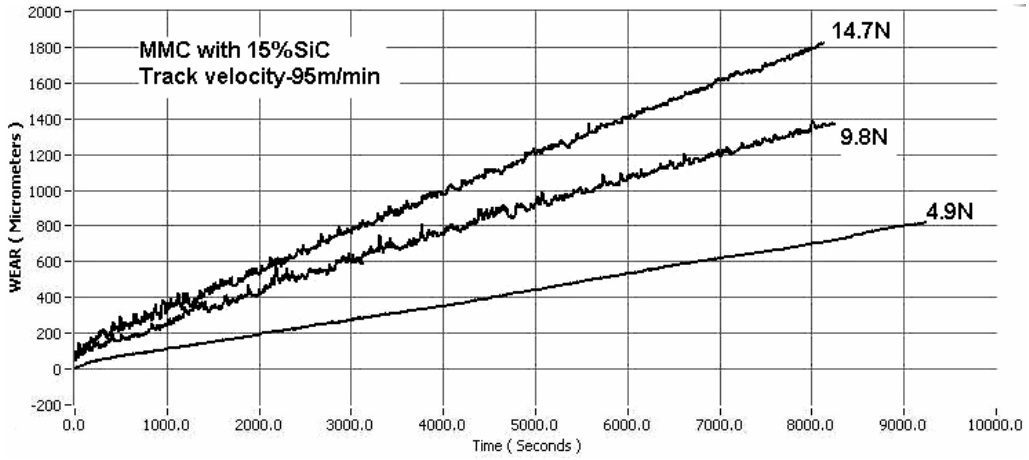

Fig. 10. Sliding wear behaviour of MMCs under different normal loads

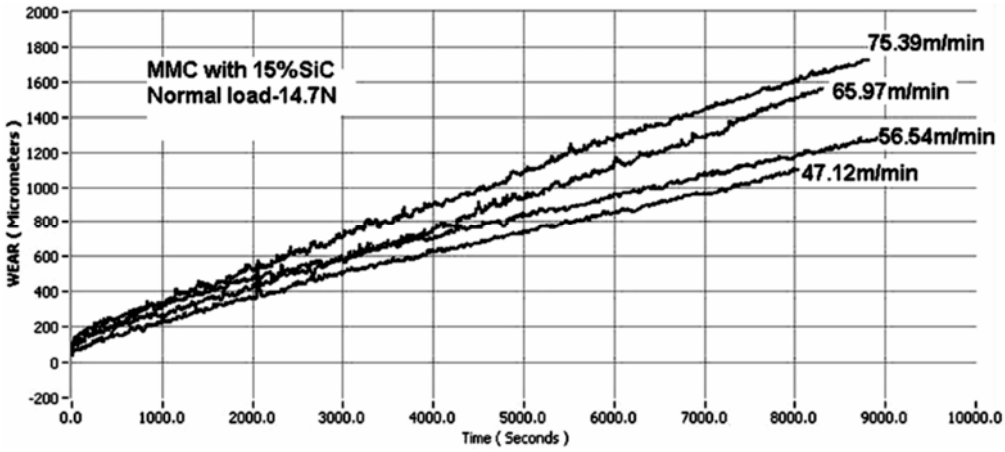

Fig. 11. Sliding wear behaviour of MMCs at different sliding velocities

Abrasion. A number of grooves, mostly parallel to the sliding direction, is evident on all the worn pins (Fig. 12). Grooving appears more severe at higher loads, 14.7N, and higher sliding velocities, 95 $m \cdot min^{-1}$ (Fig. 13). Grooves were less severe for lower loads and lower speeds. Such features are characteristics of abrasion, in which hard asperities of the steel counterface, or hard reinforced particles in between the contacting surfaces, plough or cut into the pin, causing wear by removing small fragments of material. The abrasion took place primarily via ploughing, in which material is displaced on either side of the abrasion groove without being removed, or through wedge forming, where tiny wedge-shaped fragments are worn only during initial contact with an abrasive particle [21]. The abrasion is extensive in the Al/SiC composites tested, due to the presence of dislodged and fractured SiC, which become trapped in the sliding interface and gets embedded in the counterface, contributing to three body abra-

sive wear. In addition, fractured SiC particles trapped between the sliding surfaces would also cause the abrasion of the steel disc, as would work-hardened fragments of matrix alloy and steel.

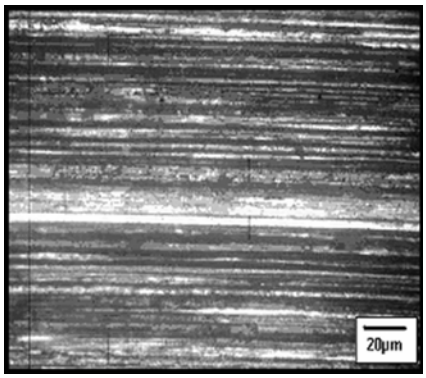

Fig. 12. Wear grooves on the worn pin surface

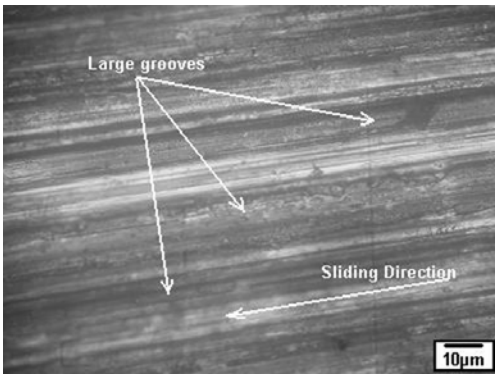

Fig. 13. Severe and large wear grooves

Oxidation. Under the optical microscope, dark surfaces are found to be covered extensively by a thin layer of fine particles (Fig. 14). Large amounts of fine powder are also present in the wear debris. These characteristics are indicative of oxidative wear, in which frictional heating during sliding causes oxidation of the surface, with wear occurring through the removal of oxide fragments [22]. Over continuous sliding, oxide wear debris fills the valleys on the pin surface and is compacted into a protective layer preventing metallic contact, and the wear rate of the composite drops accordingly [23].

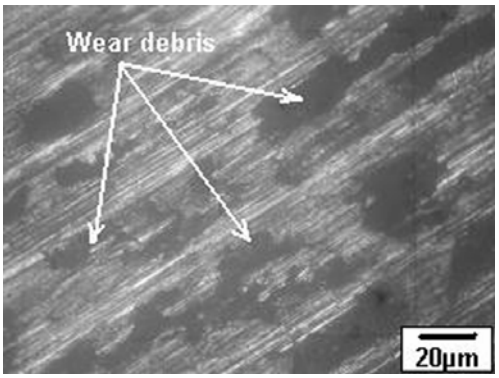

Fig. 14. Layer of oxide particles covering wear surface

Thermal softening and plastic deformation. At higher sliding speeds (95 $m \cdot min^{-1}$) and higher loads (14.7 N) material transfer is evident on the pin surfaces, indicating plastic deformation. This was observed predominantly during the wear test of the base matrix material and of MMC with a small amount of SiC.

Under the most severe sliding condition – 95m·min^{-1} and 14.7 N – associated with a longer contact time of the surfaces, gross plastic deformation of the pin surface occurs and the material is extruded from the interface before re-solidifying around the periphery of the pin as in Figure 15a. When the sliding speed and applied load reach certain critical thresholds, temperatures at contacting asperities nearly reach the melting point of the matrix alloy, causing a gradual softening of the matrix and an increasing in wear. This type of wear is predominantly observed in MMC specimens containing smaller amounts of SiC and in the base metal.

In pins tested at higher speeds and 14.7 N load, layers of material are seen protruding for the composite with 15% SiC and large protrusions can be observed for MMC with 5% SiC at the trailing edge, indicating thermal softening (Fig. 15b).

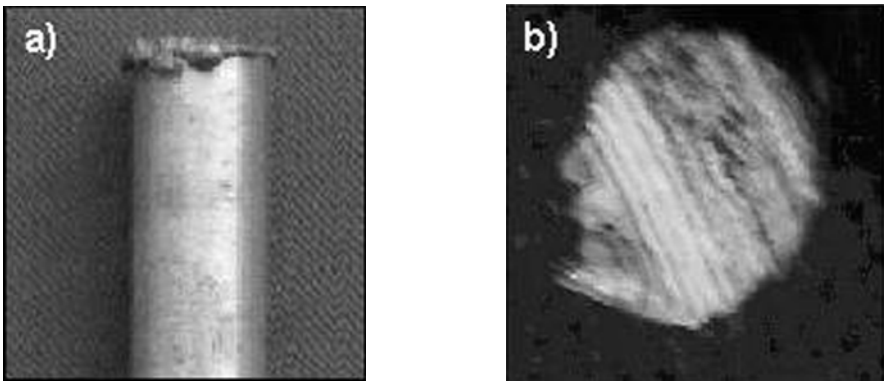

Fig. 15. Thermal softening and plastic deformation

Wear debris. The worn debris of the metal matrix composite with 15% of SiC is shown in Figure 16. A substantial quantity of wear debris was generated during the tests. The debris has three major morphologies: particle-like and flake-like aluminium, and a black powder of fractured SiC particles. A typical example of the flake type Al is shown in Figure 16a, namely flake-like wear debris obtained under 14.7 N and 95 m·min^{-1} on 15% SiC MMC specimens. These flakes have irregular shapes: some look like sponges, some are circular lumps, while some have sharp and angular features. On the other hand, Figure 16b shows flake-like aluminium debris of medium size collected from the same test. In fact, these two types of wear debris could be observed in all tests, the only difference being the relative amount of each type, and this could be influenced to a great degree by the normal load and sliding velocity. Figure 16c shows the dark powder-type mixture containing fractured SiC particles and small Al particles. As a whole, wear debris at 14.7 N load and 95 m·min^{-1} is dark in colour and mainly in the form of fine particles or flakes. At a load of 4.9 N, the debris formed consists of fine particles, which appear due to the shear fracture during the wear test. The volume of the wear debris increases with increasing normal load and sliding velocity, resulting in greater wear loss for higher loads and sliding velocities.

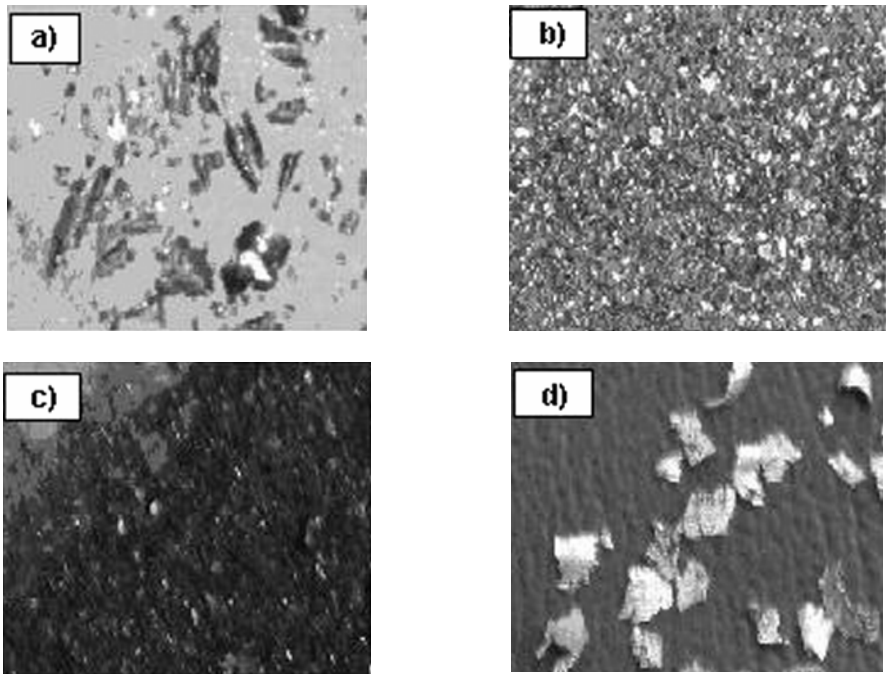

Fig. 16. Photomicrographs of wear debris

4.5. Slurry erosive wear

The results of slurry erosive wear are shown in Figure 17. The results show an increase in slurry wear resistance with increasing SiC content. Compared to the base metal, the composite with 15% SiC showed less weight loss. The presence of SiC particles essentially improved wear resistance during the initial 8–10 hours. After this time of testing, however, weight loss was found to be almost zero in all cases. The decrease in weight loss is due to the formation of a passive layer on the surface of the specimen, which retards wear by acting as a protective layer. The erosion–corrosion of MMCs usually proceeds by three different mechanisms: (i) corrosion of the matrix alloy, (ii) abrasion/erosion of the matrix as well as passive layer formation over the specimen, and (iii) fragmentation and removal of reinforcing agent dispersoids from the specimen surface by the impact of suspended erodent. Corrosion of the matrix takes place by an oxidation reaction [24], in which Al^{3+} is released from the matrix to the slurry. This results in the exposure of a large fresh area of the specimen surface to the slurry, and causes further removal of matrix alloy and hence a higher rate of weight loss during the initial stage. As time progresses, the slurry adjacent to the specimen surface becomes saturated with Al^{3+}, resulting in a reduction in the pH of the slurry. As a result, the dissolution rate of Al^{3+}in the slurry is reduced and the excess Al^{3+} is deposited over the specimen surface, which combines with OH^- to form $Al(OH)_3$ over the specimen surface. This passive layer, as long as it is not broken,

protects the matrix from direct contact with the slurry and lowers the rate of weight loss. Additionally [25, 26], the gas evolving during corrosion is entrapped in crater

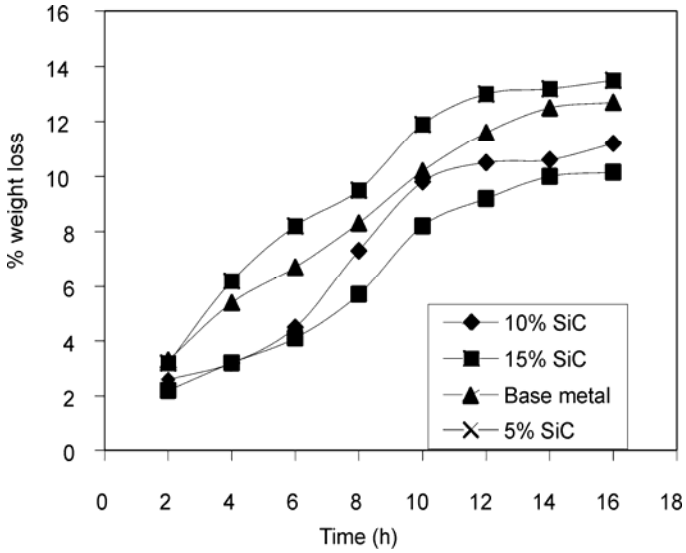

Fig. 17. Weight loss during slurry erosive wear as SiC content was varied

microsites (formed due to particulates escaping or the removal of matrix) and protects them from the slurry, which further lowers the rate of weight loss.

4.6. Fog corrosion

Figure 18 shows the results of a salt solution fog corrosion test. The resistance to corrosion is good in the non-reinforced specimens as compared to those being rein-

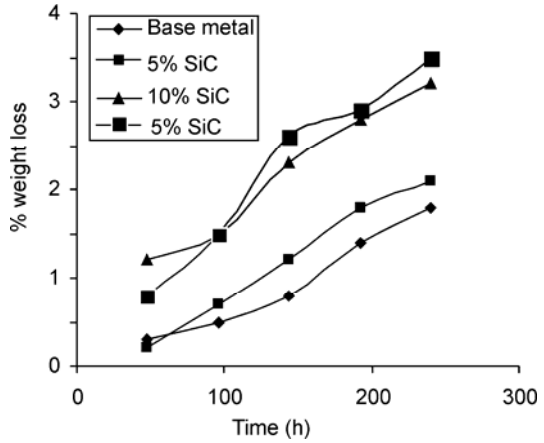

Fig. 18. Weight loss during fog corrosion test in samples with various SiC rates

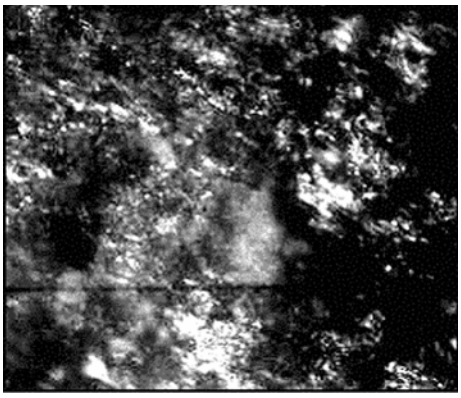

Fig. 19. Optical micrograph of corroded MMC

forced. The formation of an aluminium oxide layer is visible within 24 hours of commencing the test. The type of corrosion was found to be pitting corrosion. After 24 hours, it is observed that the formation of pit is more rapid in reinforced samples than in non-reinforced ones. SiC particles act as sites initiating pits. As is evident from Figure 19, there is a build up of corroded particle debris in the pits. Pits initiate at flaws within the surface film and at sites where the film is damaged mechanically under conditions when self-repair will not occur. Places where the matrix surface is broken on the interface between the reinforcement and the matrix will act as pit initiators. A corrosion pit is a unique type of anodic reaction and the autocatalytic process. The corrosion process within a pit produces conditions both stimulating and necessary for the continuing activity of the pit. This is illustrated schematically in Figure 20. Since pits arise at flaws, and the interface between matrix aluminium and a reinforced particle is a flaw, the metal aluminium is pitted by aerated sodium chloride solution. Rapid dissolution of aluminium occurs within a pit, while oxygen reduction takes place on adjacent surfaces. This process is self-stimulating and self propagating.

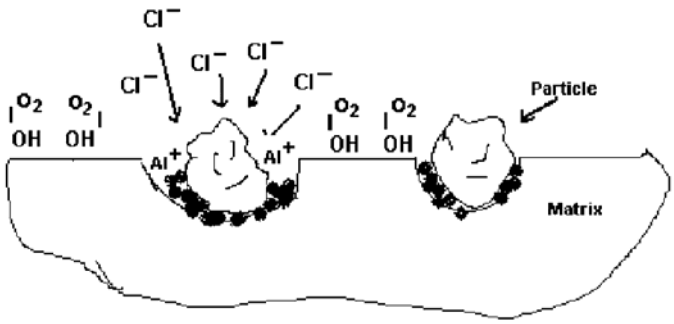

Fig. 20. Schematic autocatalytic process in pitting corrosion

A rapid dissolution of aluminium within the pit tends to produce an excess of positive charge in this area, resulting in the migration of chloride ions to maintain electro neutrality. Thus, there is a high concentration of aluminium chloride in the pit, and

a high concentration of hydrogen ions as a result of hydrolysis. Both hydrogen and chloride ions stimulate the dissolution of aluminium matrix and the entire process accelerates in time. Since the solubility of oxygen is virtually zero in concentrated solutions, no reduction of oxygen takes place within a pit. Cathodic oxygen reduction on surfaces adjacent to pits tends to suppress the corrosion there by protecting the matrix metal adjacent to the pit.

5. Conclusions

Metal matrix composites containing 5%, 10%, and 15% of SiC were synthesized successfully by the vortex method. Macrostructure and microstructure revealed a near uniform distribution of SiC particles in the centre portion of the casting. There was a slight agglomeration of SiC particles, however, on macroscopic scale. There was not much change in the density of MMC with the reinforcement of SiC particles. The bulk hardness and sliding wear resistance of MMC increase with increasing SiC content. Increasing normal load and sliding velocity increase the magnitude of wear. Different wear mechanisms were found to operate under different test conditions, varying in normal load, per cent of SiC content and sliding velocity. These are abrasion, oxidation, thermal softening, and plastic deformation. Slurry erosive wear resistance increases with increasing if SiC content. The formation of passive layers on the surface of the slurry erosive specimens decreased wear loss by forming protective layers against the impact of slurry. The corrosion resistance of reinforced samples decreases with increasing SiC content.

References

[1] SHIPWAY P.H., KENNEDY A.R., WILKES A.J., Wear, 216 (1998), 160.
[2] MA Z.Y., LIUNG Y.N., ZHANG Y.Z., LU Y.X., BI J., Mater. Sci. Tech, 12 (1996), 751.
[3] PARIMALA BAI B.N., RAMASESH B.S., SURAPPA M.K., Wear 157 (1992), 295.
[4] VENKATARAMAN S., SUNDARARAJAN S., Acta Mater., 44 (1996), 451.
[5] SATO A., MEHRAHIAN R., Metall. Trans. B, 7 (1976), 443.
[6] WANG A., RACK H.J., Mater. Sci. Eng., A247 (1991), 211.
[7] WILSON S., ALPAS A.T., Wear, 196 (1996), 270.
[8] MARTIN A., MARTINET M.A., LLORCA J., Wear, 193 (1996), 169.
[9] CHUNG S., HWANG B.H., Tribology Int., 27 (1994), 307.
[10] HUSKING F.M., FOLGAR PORTILLO F., WUNDERLIN R., MEHRABIAN R., J. Mater. Sci., 17 (1982), 477.
[11] SANNINO A.P., RACK H.J., Wear, 197 (l996), 151.
[12] SANNINO A.P., RACK H.J., Wear, 189 (1995), 1.
[13] DAS S., MONDAL D.P., DASGUPTA R., PRASAD B.K., Wear, 236 (1999), 295.
[14] SAXENA M., MODI O.P., PRASAD B.K., JHA A.K., Wear, 169 (1993), 119.
[15] MCINTYRE J.F., CONRAD R.K., GOLLEDGE S.L., Corrosion, 46 (1996), 902.
[16] TRAZASKOMA P.P., Corrosion, 46 (1996), 402.
[17] YU S.Y., ISHII H., CHUANG T.H., Metall. Mater. Trans., A 27 (1996), 2653.
[18] ROHATGI P.K., GUO R.Q., KESHAVARAM B.N., Key Eng. Mater., 104 (1995), 283.

[19] MANOHARAN S., LEWANDOWSKI J.J., Acta Metall., 38 (1990), 489.
[20] SURAPPA M.K., ROHATGI P.K., Metal Tech., 4 (1981), 41.
[21] QUINN T.J.F., J. Appl. Phys., 13 (1962), 33.
[22] STOTT F.H., WOOD G.C., Tribol. Int., 11 (1978), 211.
[23] SUH N.P., Wear 44 (1977), 1.
[24] SLREHBLOW H.H., International Congress on Metallic Corrosion, June 1984, National Research Council, Canada, 1984, p. 99.
[25] TURENNE S., SIMROD D., FIEST M., Wear, 149 (1991), 187.
[26] TURENNE S., CHATIGNY Y., SIMARD D., CARON S., MASOUNAVE J., Wear 141 (1990), 147.

Received 31 May 2005
Revised 10 July 2005